RFID-Based Localization for Greenhouses Monitoring Using MAVs

M. Longhi*, Z. Taylor†, M. Popović†, J. Nieto†, G. Marrocco*, R. Siegwart†
*University of Rome "Tor Vergata", Department of Civil Engineering and Computer Engineering (DICII), Rome, Italy
†ETH Zürich, Autonomous Systems Lab (ASL), Zürich, Switzerland

***Abstract*—This paper presents a localization method for Micro Aerial Vehicles (MAVs) equipped with RFID sensors for the monitoring of small indoor areas such as greenhouses. After validating the localization procedure, we perform some experiments aimed to produce thermal mapping in an indoor environment to control and prevent anomalous changes for the plant safety. Moreover, the accuracy of our RFID based localization method is evaluated by comparison with Maplab and Vicon systems, two precise but expensive localization method. We obtained a localization accuracy of $\sigma = 0.12\,m$ as standard deviation for the RFID localization system, that could be considered adequate for a greenhouse.**

***Index Terms*—RFID sensors, RFID localization, Micro Aerial Vehicles, Greenhouses, Precision Agriculture.**

I. Introduction

To enable Precision Agriculture (PA) practices in large greenhouse structures, a wide range of environmental parameters, such as temperature, light intensity, and humidity, must be accurately monitored to ensure optimal growing conditions for specific plants [1]. In this framework, it is crucial to know precise locations at which sensor data is collected, so that the corresponding information can be correctly associated with the affected plants (Fig 1). However, traditional manual procedures for data acquisition are labor-intensive and time-consuming, whereas standard automated methods, such as fixed Wireless Sensor Networks (WSN) [2] based on fixed monitoring locations, are costly to deploy in large indoor spaces. Recently, Micro Aerial Vehicles (MAVs) have emerged as a flexible, cost-efficient alternative. Equipped with Radio Frequency IDentification (RFID) tags or readers, these systems have the potential to achieve an efficient pervasive monitoring for a variety of indoor spaces [3].

MAVs are rapidly gaining popularity for a broad range of applications, including environmental monitoring [4]–[6]. In PA, these devices have been deployed for various tasks, e.g., monitoring vegetation density [7], irrigation planning and water stresses [8], and weed detection [9] on farms. For indoor farming in greenhouses [10], where the dimension of the perimeter to be controlled is reduced, all standard solutions are too expensive. These MAV systems can utilize localization and mapping approaches, such as Maplab [11], to produce high-quality spatial maps of these environments by integrating onboard camera and inertial measurements. However, low-cost, extremely light weight systems are not equipped with sufficient computational power to run these localization approaches online. To overcome this, we propose an alternative localization system based on the electromagnetic interrogation of a grid of low-cost RFID tags with known positions. This tag-based approach enables localization in indoor environments and after a mission, the system can transfers its recorded data to a Ground Station (GS) to create a 3D-map with accurate information about both the trajectory and the environmental variable of interest [12].

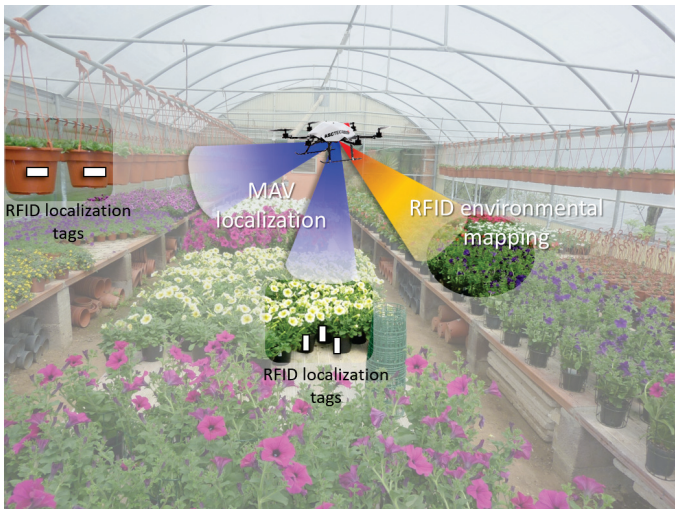

Figure 1. MAV & RFID for monitoring in greenhouses.

The aim of this work is to enable environmental mapping and localization procedures with a light weight, low-cost MAV in PA-GPS-denied locations such as small-scale greenhouses [13]. To validate our method, we consider the possible application of temperature mapping. At this purpose, we firstly apply the common method of a computationally demanding, but more accurate, Visual-Inertial (VI) mapping system incorporating sensory information, then a simple but efficient, RFID based localization approach is presented.

Preliminary results of VI-based temperature mapping and our localization approach are finally presented.

II. Method

In this section we are going to present the theoretical background of our proposed method both for the creation of

978-1-5386-6765-1/18/$31.00 ©2018 IEEE

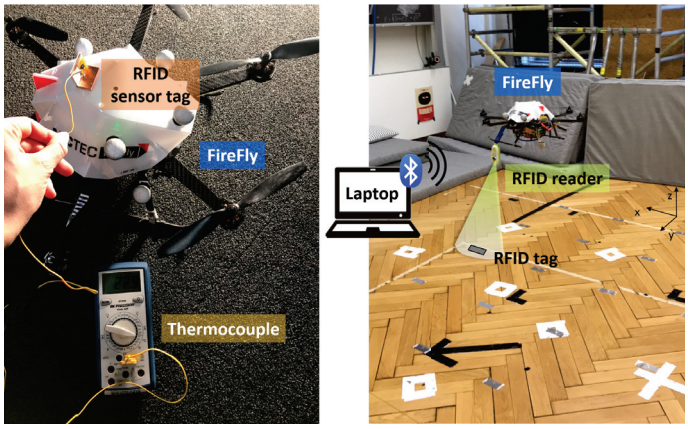

(a) (b)

Figure 2. (a) The FireFly MAV equipped with the RFID temperature sensor, which acquired data are compared to a thermocouple and (b) the same MAV equipped with the qIDmini RFID reader flying over a grid of passive RFID tags attached on the floor.

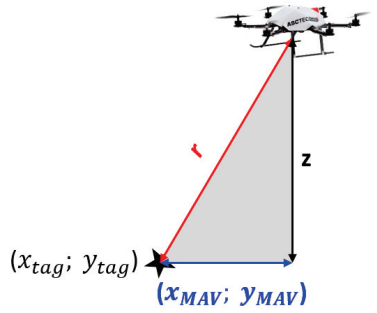

Figure 3. A schematic for estimating the MAV pose. The distance of the reader, mounted on the MAV, to the tag is computed through the RSSI response, while the x and y positions are calculated through the tag read region, using the footprint formula.

3D-temperature map with the RFID sensor and for indoor path planning using RFID passive tags.

A. RFID Temperature Maps

When a MAV flies inside a greenhouse is useful if the collected temperature data can be reconstruct as a 3D-map. Correlate environmental samples with the effective position of such measurements allow an intervention in case of anomalies or necessity. To validate this idea, during the MAV flight, the temperature, IMU and camera data are collected and, the map is reconstructed in post-processing using Maplab tools.

Fig. 2(a) depicts our experimental setup to map temperature in an indoor environment. A Battery Assisted Passive (BAP) RFID tag working as a data-logger [14], is mounted on the top cover of the MAV to avoid propeller disturbances during temperature measurements. The particular shape of the RFID antenna connected to the SL900A microchip is designed to be adapted for a wide range of MAV platform types and sizes, from nano-MAVs with very limited payload to small multi-rotor air frames. The sensor dimensions are $4 \times 4 \times 2\,cm$, and its weight is $12.3\,g$ [15]. The minimum sampling frequency is $1\,Hz$, with the integrated EEPROM capable of storing up to 841 samples. The embedded sensor returns a temperature in the range $40°C < T < 150°C$ with a resolution of $0.1 - 0.2°C$. Our MAV platform is an AscTec Firefly, with a rotor-to-rotor length of $45\,cm$ and maximum payload of $3\,kg$. The system is equipped with cameras and Inertial Measurement Unit (IMU) to collect state estimation and localization information during the flight.

B. RFID Localization

For the monitoring of greenhouses cultures, the localization system only requires a short-range action. To reduce costs and computational complexity, the localization can be performed using the RFID technology, embedding low-cost passive RFID tags not only on the floor but also in the plants vases of the greenhouse. In this context, a short-range reader, with limited power and costs can be used. Our experimental setup for RFID localization (Fig. 2(b)) consists of a MAV equipped with a portable qIDmini RFID reader with a maximum transmitting power of $500\,mW$ and an integrated linear antenna. The reader requires a Bluetooth wireless connection to the GS (in our case, a laptop) to transfer information collected from the tags and elaborate them. Te reference tags are Avery Dennison AD-663 dipoles, a Gen2 UHF RFID inlay suitable for a wide variety of RFID applications with a chip sensitivity of $p_c = -18\,dBmW$.

A MAV localization requires the detection of the trajectory on the 3D-space, which add a grade of complexity on the usual autonomous vehicle plane localization. Using the RFID technology, we adopt the combination of a trilateration algorithm along the x- and y-plane, together with the Received Signal Strength Indicator (RSSI) [16] used to calculate the MAV flying distance. When a tag is detected, the reading retrieves both the RSSI and the ID: while, the distance of the MAV from a responding tag (r, in Fig.3) is not directly available (we will use the RSSI formula to determine it), the ID, instead, is connected to the tag coordinates (x and y).

A key requirement in developing the localization system is the knowledge of the tag positions, which is necessary to extract the projection of the MAV on the x-y plane, i.e., the MAV pose is estimated using the footprint formula and concept [17]. The i-*th* tag is detected when the MAV lies within its corresponding read region. The shape and size of this region depend on the radiated power and electromagnetic characteristics of the reader and tags antennas. As shown in Fig. 4(a), the floor of our experimental set-up features a grid of tags, where the read region of each tag has the shape of a regular ellipsoid [18]. A tag detection means that the reading ellipsoid of the major axes d (Fig. 4(a)) is intercepted by the z-plane on which the tag is placed, i.e., the floor [3], to form the ground footprint F:

$$F(z) = \frac{2f}{d}\sqrt{2zd - 2z^2}, \tag{1}$$

where f is the minor axis of the reading ellipsoid, the

maximum range d of the reader coincides with twice the major half-axis of the reading ellipsoid and z is the MAV flying distance. By considering the footprint of each tag, the floor can be tessellated into individual cells, as shown in Fig. 4(b). The optimal flight height ($d_{opt} = 1\,m$) is chosen such that footprint size is maximized ($F_{MAX} = 60\,cm$). Flying at this optimal level with the tags evenly distributed on the floor enables multiple tags to be read simultaneously. Adding more observations, the reader location can be determined more accurately based on the circle intersections.

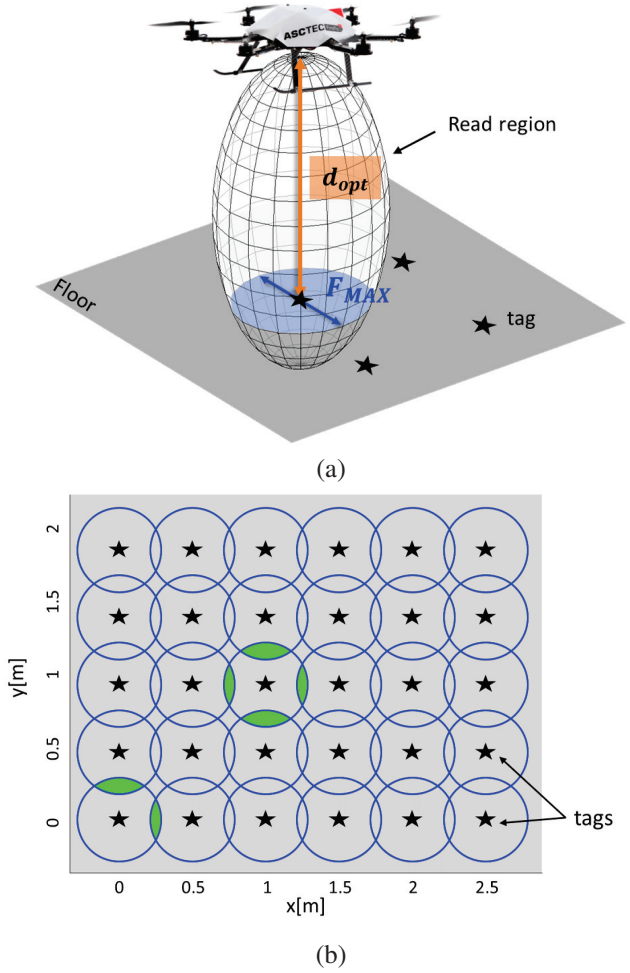

Figure 4. (a) Three-dimensional view of the MAV with the reader. Stars reperesent tags on the floor which can be detected by a MAV flying within a circle of diameter F. (b) Regions in which the floor is divided. The green areas indicate locations from which the MAV can detect more tags if it flies at a distance d_{opt} from the floor.

The altitude of the MAV is estimated from the reflected RSSI signal returned by the reader for each tags. The red hypotenuse line of Fig. 3 is the effective distance of the MAV from a detected tag, which can be approximated to z (Pythagoras formulas). The absolute distance r (i.e. the altitude) between MAV and tags can be hence estimated using the RSSI and path-loss propagation models [19]:

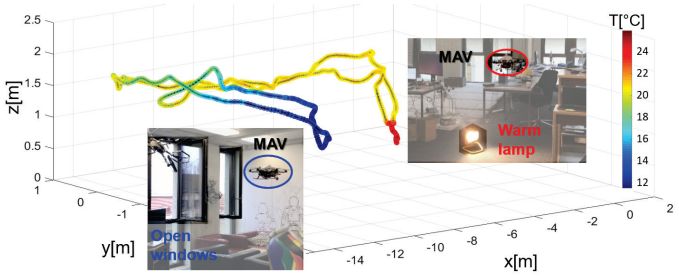

Figure 5. Example ofthe 3D-reconstruction of the temperature map from our flight experiment. The minimum and maximum temperature levels recorded are 11°C (blue) and 24°C (red).

$$RSSI = -10nlog_{10}(r/r_0) + A, \tag{2}$$

where n is the path loss exponent, which varies from 2 in free space to 4 in indoor environment, r_0 is usually $1\,m$ as a standard reference distance, and A is the RSSI value at a reference distances from the reader. This value is approximated during the calibration phase, i.e. by collecting RSSI data from different distances and averaging the signal strength measurements at each step.

III. Experimental Tests

We did experiments to (i) create a spatial-temporal environmental map in an indoor environment by introducing a huge temperature gradient for test the reliability of the sensor in presence of temperature changes, while the MAV is using the most common VI sensors to collect the path data, and (ii) to validate RFID localization as a proof of concept for the suitability of the short-range system in greenhouses environments.

Our first aim (i), is to create an accurate temperature map with BAP RFID tag embedded on the MAV. Temperatures are sampled at $2\,Hz$ as the VI system gathers mapping data. We performed the experiment in the corridor of the ETH Autonomous Systems Lab, using a warm lamp to heat a small area locally, and open windows on a snowy day to cool one corridor end. As the heating effect is localized, we expect the breeze from outdoors to spread quickly within the environment. Fig. 5 illustrates the resulting temperature map, which correctly reflects the environmental setup with a range variation of more than $10°C$.

After validating the environmental map system, our second experiment (ii) envolved the MAV equipped with the portable qIDmini RFID reader directly attached to one of its legs. The MAV was driven manually flying at different altitude (less than $2\,m$) from the ground. The reader emits electromagnetic beacons with a power of $27\,dBmW$ to a 6×5 grid of passive tags as the MAV navigates over them. The distance between tags is chosen based on the optimal reading distance d, tags are evenly distributed on the floor at a distance of $50\,cm$ each other in both x and y directions, to enable multiple tags to be read simultaneously at times. Fig. 6 shows the resulting spatial

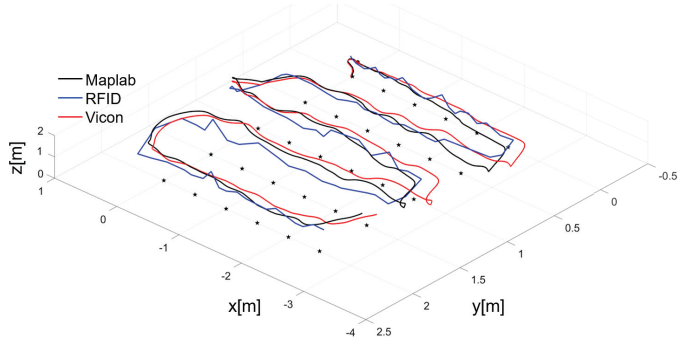

Figure 6. Results from our localization system experiments. Blue and black show the path reconstructed by RFID values and the camera path, respectively, while the ground-truth, acquired from the Vicon system, is indicated in red. When the MAV flies over multiple tags, altitude is computed from the reflected power level.

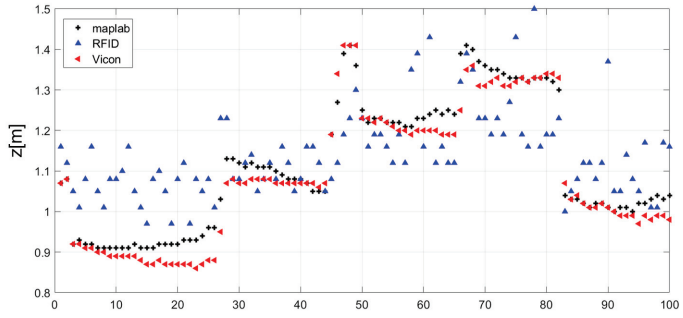

Figure 7. The accuracy the path planning experiment, along the z-axis, is valuated comparing to the standard deviation.

map. The RSSI values collected by the RFID system are used to calculate altitude at each reading instant.

To evaluate accuracy along the z axis (Fig. 7), we relate the precision of Maplab and RFID systems to Vicon [20] data (assumed as the ground-truth) through the standard deviation index. Smaller values of in relation to the ground-truth value indicate a lower measurement variance, and thus higher precision. In our experiments, the indices for Maplab and RFID data were calculated as $\sigma_{Maplab} = 0.03\,m$ and $\sigma_{RFID} = 0.12\,m$. We also consider the variation coefficient σ^2 as a relative index to compare the dispersion of data with different types, regardless of their absolute quantities. Results of $\sigma^2_{Maplab} = 5\%$ and $\sigma^2_{RFID} = 10\%$, confirm that our RFID system is suitable of reliable greenhouses when the accuracy is of the plant order.

IV. Conclusion

This paper presents a low-cost RFID system for MAV localization in indoor environments, such as greenhouses, and its application to collect accurate temperature data with an on-board RFID tag antenna. Preliminary experiments were performed to validate our proposed system, noting that our approach is applicable for other environmental monitoring scenarios, e.g., humidity, light intensity, etc. The system evaluation demonstrates an $50\,cm$ resolution of our low-close, simple RFID solution, which is suitable for greenhouse applications.

References

[1] D.D. Chaudhary, S.P. Nayse, L.M. Waghmare, "Application of Wireless Sensor Networks for Greenhouse Parameter Control in Precision Agriculture," International Journal of Wireless & Mobile Networks (IJWMN), Vol. 3, No. 1, pp. 140-149, 2011.

[2] I.F. Akyildiz, W. Su, Y. Sankarasubramaniam, E. Cayirci , "Wireless Sensor Networks: a Survey," Computer Networks, Vol. 38, No. 4, pp. 393-422, 2002.

[3] M. Longhi, et al., "RFIDrone: Preliminary Experiments and Electromagnetic Models," URSI International Symposium on Electromagnetic Theory (EMTS), pp. 450-453, 2016, Espoo, Finland.

[4] "Unmanned Aerial Vehicles for Environmental Applications," International Journal of Remote Sensing, Taylor & Francis, Inc. Bristol, PA, USA, vol. 38, issue 8–10, pp. 2029–2036, 2017.

[5] C. Zhang, J. M. Kovasc, "The Application of Small Unmanned Aerial Systems for Precision Agriculture: a Review," Precision Agriculture, Vol. 13, No.6, pp. 693-712, 2012.

[6] M. Popovic, T. Vidal-Calleja, G. Hitz, I. Sa, R. Siegwart, J. Nieto, "Multiresolution Mapping and Informative Path Planning for UAV-based Terrain Monitoring," arXiv preprint arXiv:1703.02854, 2017.

[7] J. Primicerio, et al., "A Flexible Unmanned Aerial Vehicle for Precision Agriculture," Precision Agriculture, Vol. 13, No. 4, pp. 517-523, 2012.

[8] P.J. Zarco-Tejada, V. González-Dugo, J.A. Berni, "Fluorescence, temperature and narrow-band indices acquired from a UAV platform for water stress detection using a micro-hyperspectral imager and a thermal camera," Remote Sensing of Environment, Vol. 117, pp. 322–337, 2012.

[9] J. Valente, D. Sanz, J. del Cerro, A. Barrientos, M.A. de Frutos, "Near-optimal coverage trajectories for image mosaicking using a mini quadrotor over irregular-shape fields," Precision Agriculture, Vol. 14, pp. 115–132, 2013.

[10] E. SF. Berman, et al., "Greenhouse gas analyzer for measurements of carbon dioxide, methane, and water vapor aboard an unmanned aerial vehicle," Sensors and Actuators B: Chemical, Vol. 169, pp. 128-135, 2012.

[11] T. Schneider, et al., "maplab: An Open Framework for Research in Visual-inertial Mapping and Localization," arXiv preprint, 2017.

[12] M. Longhi, et al., "An Integrated MAV-RFID System for Geo-referenced Monitoring of Harsh Environments," In Proc. of the International Conference on Antenna Measurement and Applications, IEEE CAMA.

[13] J. J. Roldan, et al., "Mini-UAV Based Sensory System for Measuring Environmental Variables in Greenhouses," Sensors, Vol. 15, No. 2, pp. 3334-3350, 2015.

[14] M. Longhi, G. Marrocco, "Ubiquitous Flying Sensor Antennas: Radiofrequency Identification Meets Micro Drones," RFID IEEE Journal of Radio Frequency Identification, Vol. 1, No. 4, pp. 291-299, 2018.

[15] M. Longhi, G. Marrocco, "Flying Sensors: Merging Nano-UAV with Radiofrequency Identification," IEEE 2017 RFID-TA, September 2017, Warsaw, Poland.

[16] F. J. Highton, "Received Signal Strength Indicator," U.S. Patent, No. 4, 578, 820, 25 March 1986.

[17] G. Marrocco, E. Di Giampaolo, R. Aliberti, "Estimation of UHF RFID Reading Regions in Real Environments", IEEE Antennas and Propagation Magaz., Vol. 51, pp. 44-57, Dec. 2009.

[18] G. Casati, et al., "The Interrogation Footprint of RFID-UAV: Electromagnetic Modeling and Experimentations," RFID IEEE Journal of Radio Frequency Identification, Vol. 1, No. 2, pp. 155-162, 2017.

[19] P. Kumar, L. Reddy, S. Varma, "Distance measurement and error estimation scheme for rssi based localization in wireless sensor networks," in Wireless Communication and Sensor Networks, pp. 1–4, IEEE, 2009.

[20] L. Heng, L. Meier, P. Tanskanen, F. Fraundorfer, M. Pollefeys, "Autonomous obstacle avoidance and maneuvering on a vision-guided mav using on-board processing," In Proc. of the IEEE Int. Conf. on Robotics and Automation (ICRA), pp. 2472–2477, 2011.